applied optics

783 nm wavelength stabilized DBR tapered diode lasers with a 7 W output power

Bernd Sumpf,* Lara Sophie Theurer, Martin Maiwald, André Müller, André Maaßdorf, Jörg Fricke, Peter Ressel, and Günther Tränkle

Ferdinand-Braun-Institut gGmbH, Leibniz-Institut für Höchstfrequenztechnik, Gustav-Kirchhoff-Str. 4, Berlin 12489, Germany
**Corresponding author: bernd.sumpf@fbh-berlin.de*

Received 12 February 2021; revised 29 April 2021; accepted 21 May 2021; posted 24 May 2021 (Doc. ID 422688); published 17 June 2021

Wavelength stabilized distributed Bragg reflector (DBR) tapered diode lasers at 783 nm will be presented. The devices are based on GaAsP single quantum wells embedded in a large optical cavity leading to a vertical far field angle of about 29° (full width at half maximum). The 3-inch (7.62 cm) wafers are grown using metalorganic vapor phase epitaxy. In a full wafer process, 4 mm long DBR tapered lasers are manufactured. The devices consist of a 500 μm long 10th order surface DBR grating that acts as rear side mirror. After that, a 1 mm long ridge waveguide section is realized for lateral confinement, which is connected to a 2.5 mm long flared section having a full taper angle of 6°. At an injection current of 8 A, a maximum output power of about 7 W is measured. At output powers up to 6 W, the measured emission width limited by the resolution of the spectrometer is smaller than 19 pm. Measured at $1/e^2$ level at this output power, the lateral beam waist width is 11.5 μm, the lateral far field angle 12.5°, and the lateral beam parameter M^2 2.5. The respective parameters measured using the second moments are 31 μm, 15.2°, and 8.3. 70% of the emitted power is originated from the central lobe.

https://doi.org/10.1364/AO.422688

1. INTRODUCTION

Diode lasers in the spectral range around 785 nm are requested, e.g., as pump lasers for 2 μm eye-safe Tm:YAG lasers [1,2] and as excitation light sources for Raman spectroscopic experiments with wide area excitation [3]. Here, the output power should be adjusted to the size of the illuminated area and provide the necessary power density at the sample under study. For areas with diameters in the millimeter range and larger, the laser power could be in the range of several watts.

Beside this, the laser should provide a wavelength stabilized and narrowband emission. For the pumping of Tm:YAG, two pronounced absorption features at 781 nm and 786 nm are preferable [2], i.e., the pump source should emit within this range. For Raman spectroscopy and the detection of Stokes shifted Raman lines, the wavelength of the excitation light source should be just below the cut-on wavelength for available long-pass filters at 785 nm. In the latter case, due to the width of the Raman lines of solids and liquids [4], which is typically below 0.6 nm (10 cm^{-1}), also requirements for the emission width have to be taken into account. Besides the power and spectral requirements, a good beam quality could enable Raman measurement systems with a multimode fiber optical probe, and fiber coupled diode laser modules could be used for the above pumping application [5].

Broad area lasers with a stripe width of 95 μm emitting at 790 nm reach an output power up to 9 W, showing high reliability [6]. Nevertheless, the spectral width is in the range of 1.5 nm, and the beam propagation ratio is larger than 10. For distributed feedback (DFB) broad area lasers, wavelength stabilized output powers up to 1.4 W were reported by Maiwald *et al*. [7]. Their applicability in Raman spectroscopic measurements were demonstrated by Ahmad *et al*. [8].

Wavelength stabilized and diffraction limited devices in the low power range up to 200 mW suitable for Raman spectroscopy were reported by several groups. DFB ridge waveguide (RW) lasers at 780 nm with an output power of about 10 mW were presented, e.g., by Inoguchi *et al*. [9] and with 200 mW by Wenzel *et al*. [10].

DBR-RW lasers at 780 nm were reported by Jiang *et al*. [11]. The devices reached an optical output power up to 110 mW. In our group, DBR-RW lasers with higher order surface gratings for wavelength stabilization with output powers up to 215 mW having a narrow spectral line width were manufactured [12]. Recently, higher output powers up to 500 mW were achieved in a hybrid master oscillator power amplifier configuration maintaining the diffraction limited beam quality [13].

A well-established concept for further increase in output power together with a near diffraction limited power are tapered lasers as reported, e.g., by Walpole [14], Mikulla *et al.* [15],

and by our group [16]. Output powers up to 15.5 W were reached for DBR tapered lasers at 1030 nm based on InGaAs triple quantum wells embedded into a 4.8 μm wide asymmetric large optical cavity [17].

In this work, DBR tapered diode lasers emitting at 783 nm will be presented. They are based on a vertical structure having a GaAsP single quantum well (SQW) as the active region and a waveguide thickness of 1 μm. The material data of this structure, the lateral design, and the processing of the laser diodes will be presented. The power–voltage–current characteristics show a maximal output power of 7 W in continuous wave operation. Spectral data will be presented with a measured emission width below 19 pm limited by the resolution of the spectrometer. Beam quality measurements show that about 70% of this output power is emitted from the central lobe up to an output power of 6 W. The lateral beam propagation ratio measured at $1/e^2$-level is determined to 2.5; measured as second moments, it is 8.3. To the best of our knowledge, this is the highest wavelength stabilized power reported for a monolithic DBR tapered laser at 783 nm together with an improved beam quality.

2. VERTICAL LAYER STRUCTRE

The vertical layer structure was grown using metalorganic vapor phase epitaxy (MOVPE). A scheme of the structure is shown in Fig. 1. The active region is formed by a 14 nm thick GaAsP SQW embedded into 500 nm thick p- and n-waveguide layers of $Al_{0.65}Ga_{0.35}$ As. The doping in the waveguide layers was increased from the undoped SQW to about 5×10^{17} cm^{-3} at the border to the 1000 nm thick $Al_{0.7}Ga_{0.3}$ As p- and n-cladding layers.

The decision to use tensile-strained GaAsP SQW embedded in AlGaAs is based on the results of Erbert *et al.* [18] and Knauer *et al.* [19]. For these structures emitting around 785 nm, a high differential modal gain was predicted and measured. Additionally, at the facets, the relaxation of the tensile strain can lead to a non-absorbing region increasing the maximal output power and improving reliability. This well-proven structure combines an adequate small vertical far field angle with good material data. A further increase in waveguide thickness for structures in this spectral range would cause a deterioration of the material data and complicate the manufacturing of surface gratings.

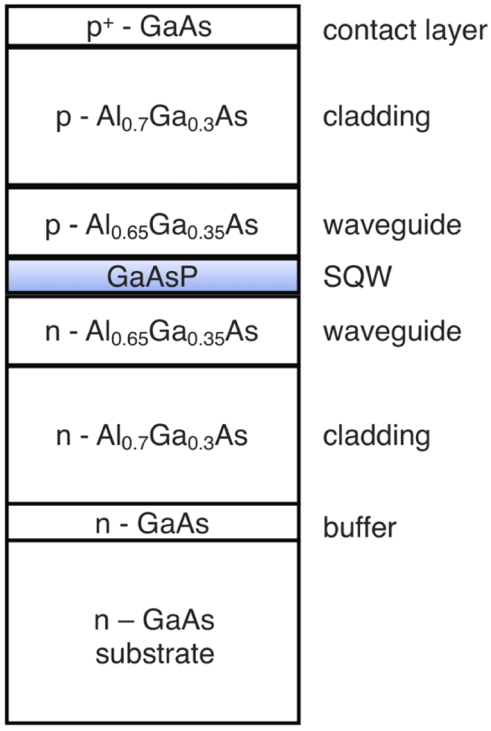

Fig. 1. Scheme of the vertical layer structure for the 783 nm DBR tapered lasers.

Uncoated 100 μm stripe width devices with different lengths L between 1000 μm and 6000 μm were measured in pulsed mode (1 kHz, 1 μs). Devices with a resonator length $L = 1000$ μm have a threshold current $I^{\mathrm{th}} = 230$ mA, a slope efficiency $S = 0.67$ W/A, and a characteristic temperature of the threshold current $T_0 = 140$ K.

The material data were determined from measurements of the threshold current I^{th} and the slope efficiency S. The determination of the internal losses α_i and the internal efficiency η_i can be performed using the following equation (η_D, differential efficiency; h, Planck's constant; ν, frequency; q, elementary charge; S, slope efficiency; R, facet reflectivity):

$$\frac{1}{\eta_D} = \frac{h \cdot \nu}{2 \cdot q \cdot S} = \frac{1}{\eta_i}\left[1 + \frac{\alpha_{\mathrm{i}} \cdot L}{\ln(1/R)}\right]. \tag{1}$$

The respective plot is shown in Fig. 2. From the zero crossing of the plot, the internal efficiency η_i was determined to (0.93 ± 0.01). The internal losses were determined to $\alpha_i = 0.91$ cm^{-1} using the slope S.

The parameters modal gain coefficient Γg_0, threshold current density for infinite cavity length $j^{\mathrm{th}}(\infty)$, and the transparency current density j^{tr} were determined using the following dependencies. As value j_0, the threshold current j^{th} (6000 μm) was used:

$$\ln\left(\frac{j_{\mathrm{th}}}{j_0}\right) = \frac{\ln(1/R)}{\Gamma \cdot g_0} \cdot \frac{1}{L} + \ln\left(\frac{j_{\mathrm{th}}(\infty)}{j_0}\right), \tag{2}$$

$$j_{\mathrm{tr}} = j_{\mathrm{th}}(\infty) \cdot \exp\left(-\frac{\alpha_{\mathrm{i}}}{\Gamma \cdot g_0}\right). \tag{3}$$

Figure 3 shows the obtained result. The calculated transparency current density is $j\mathrm{tr} = 115$ A/cm^2, and the threshold current for devices with an infinite length is $j^{\mathrm{th}}(\infty) = 122$ A/cm^2. The modal gain coefficient is determined to $\Gamma g_0 = 18$ cm^{-1}.

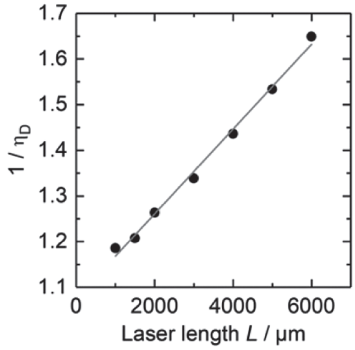

Fig. 2. Inverse differential efficiency versus laser length.

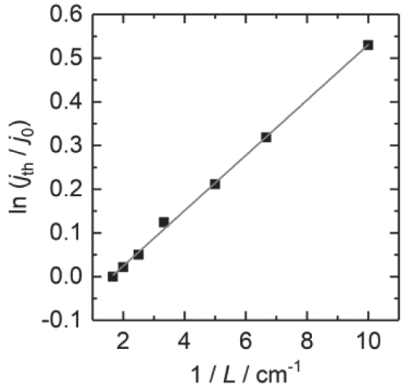

Fig. 3. Logarithm $\ln(j^{\text{th}}/j_0)$ versus inverse laser length.

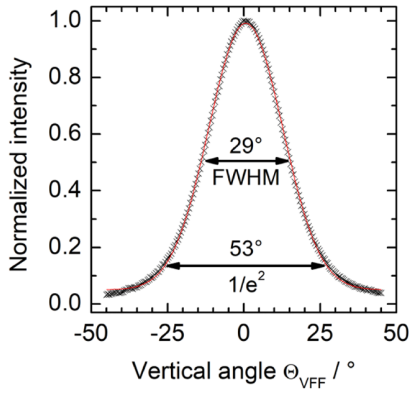

Fig. 4. Vertical far field distribution of the 783 nm layer structure given in Fig. 1.

The vertical far field distribution is given in Fig. 4. It has a Gaussian shape with a full angle measured at half maximum (FWHM) of 29° as expected for devices with a 1 μm thick waveguide. 95% of the power is emitted within an angle of 53° ($1/e^2$-level). In vertical direction, the beam has a near diffraction limited beam quality with an estimated beam propagation ratio of $M^2_{\text{vert}} = 1$.

3. LATERAL DESIGN AND PROCESSING

A top view scheme of the DBR tapered laser is given in Fig. 5. The laser length is set to $L = 4$ mm. For wavelength stabilization a 10th order DBR grating with a length of $L_{\text{DBR}} = 500$ μm is implemented at the rear side of the device. The grating has a lateral tapered design and is manufactured using electron beam lithography. At the rear end, the DBR grating has a width of 10 μm, and at the connection to the RW, the lateral tapered design ends with a width of 2.2 μm. This shape ensures a high reflectivity of the grating of about 70% for TE polarized devices as described in Ref. [17]. For the presented TM polarized structure, a reflectivity of 30% was estimated based on measurements.

A SEM picture of a part of the grating is shown in Fig. 6. The width of the trenches is about 150 nm, and the etching depth is 1470 nm. The distance between the trenches is about 1215 nm. When operating the device, the DBR section is unpumped.

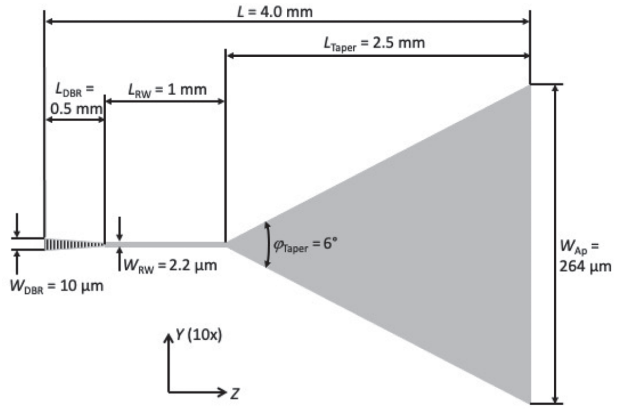

Fig. 5. Top view scheme of the 783 nm DBR tapered laser; for clarity, the y direction is magnified by a factor of 10 in comparison to the z direction.

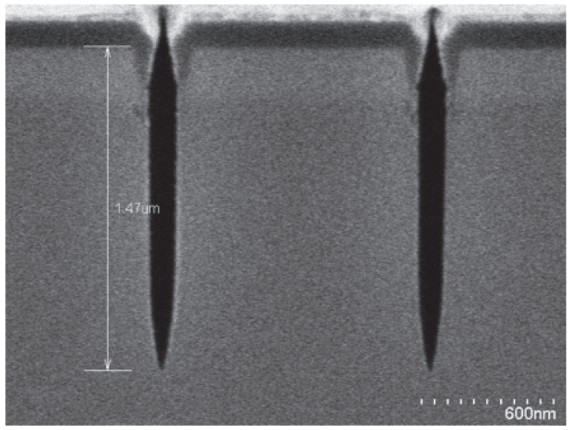

Fig. 6. SEM picture of the DBR grating.

No additional measures were taken to avoid absorption in this section.

The RW has a length of $L_{\text{RW}} = 1$ mm and a width of $W_{\text{RW}} = 2.2$ μm. The etching depth is about 1500 nm leading to an effective index step of 3×10^{-3}. This lateral waveguide design ensures single transverse mode operation.

The flared section has a length of $L_{\text{Taper}} = 2.5$ mm and a full taper angle of $\varphi_{\text{TR}} = 6°$. The output aperture has a width of $W_{\text{Ap}} = 264$ μm. For separate excitation, an isolation gap with a length of about 100 μm between the contact of the RW and the tapered section was implemented.

The structure was manufactured using i-line wafer stepper lithography. The taper is defined by implantation. For the suppression of spurious spatial modes beside the RW, also a deep implantation was used.

The lasers were cleaved to the length $L = 4$ mm, and afterwards the facets were passivated as described by Ressel *et al.* [20]. The front facet was coated with a reflectivity of $R_f = 0.2\%$ and the rear side with an anti-reflection coating of 5×10^{-4}.

The devices were mounted epi-side up on CuW using AuSn. The subassemblies were mounted on a conduction cooled gold plated copper block having a footprint of 25 mm × 25 mm. The injection current at the RW section and the tapered section can be individually controlled. In the case of the RW section, the

p-contact was formed by wire bonding. At the tapered section, a small CuW plate was soldered on top for better current and heat dissipation, and the p-contact was afterwards formed by wire bonds.

4. ELECTRO-OPTICAL DATA

In Fig. 7, the power–voltage–current characteristics of a device in continuous-wave operation at a heat sink temperature of $T = 25°C$ are shown. Here and for all further experiments, the RW section was operated with an injection current of $I_{RW} = 300$ mA. Lasing starts at a current at the tapered section of $I_{Las} = 360$ mA. The output power increases with a slope efficiency of $S = 1.1$ W/A. The calculated conversion efficiency has its maximum at $I_{Taper} \approx 4$ A with $\eta_C = 0.55$. Please note that this value does not include the electrical power for the RW section of about 0.6 W. Taking this value into account, a reduction in conversion efficiency to about $\eta_C \approx 0.50$ has to be stated. At a taper current of $I_{Taper} = 8$ A, an optical output power of $P = 7$ W was measured. For output powers larger than 5 W, an onset of a roll-over can be observed accompanied by a significant reduction in conversion efficiency.

To the best of our knowledge, this output power for tapered devices using GaAsP quantum wells is significantly larger compared to already published data for devices at, e.g., 735 nm [21] or 808 nm [22].

The dependence of the emission wavelength on the taper current is given in Fig. 8. The spectra were recorded with a double echelle monochromator DEMON from LTB Berlin, having a spectral resolution at this wavelength of about 10 pm and a dynamic range of 16-bit.

The maximum intensity of each spectrum is normalized to one, and the spectra are presented in a false color contour plot. When lasing starts, the emission wavelength has its maximum at $\lambda_{Las} = 782.73$ nm. With increasing current, the wavelength shifts towards longer wavelengths and reaches a value of $\lambda = 782.95$ nm at $I_{Taper} = 8$ A. The overall spectral tuning rate measured between 1.0 A and 6.5 A is $\Delta\lambda_{total}/\Delta I_{Taper} = 0.022$ nm/A. Characteristic mode hops

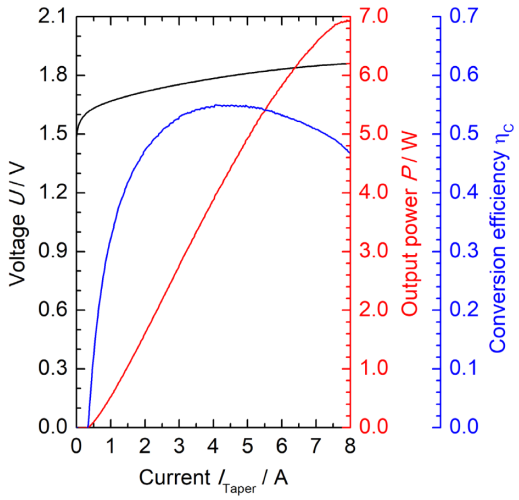

Fig. 7. Power–voltage–current characteristics for a DBR-tapered laser at a heat sink temperature of 25°C and a current through the RW section of 300 mA.

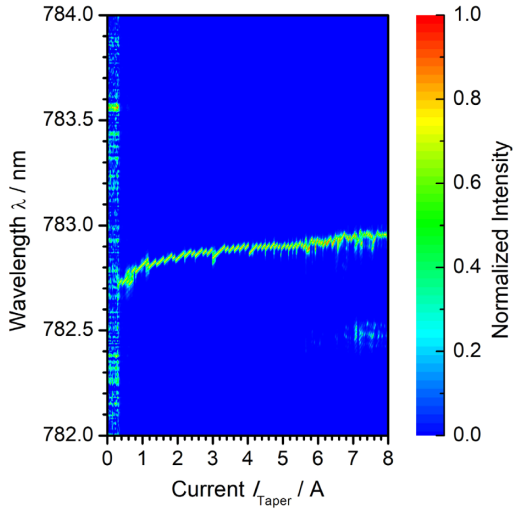

Fig. 8. Dependence of the emission wavelength on the taper current for the device in Fig. 7 at a heat sink temperature of 25°C.

typical for DBR lasers can be clearly observed. The measured spectral distance between the mode hops at currents smaller than 5 A is about $\Delta\lambda = 21$ pm. Assuming a Fabry–Perot resonator between rear and front facets of the device, this is in good agreement with the laser length of 4 mm. This value indicates a rather large transmission of the grating section and a high penetration depth of the light. The tuning within one DBR mode is $\Delta\lambda_{DBR}/\Delta I_{Taper} = 0.18$ nm/A. For larger currents, the spectral distance between the mode hops decreases, which might be a hint at thermal lensing.

From a threshold up to a current of 6.8 A, i.e., at an output power up to 6.4 W, the emission of the device shows a single dominant mode with a spectral width of about $\Delta\lambda_{FWHM} \approx 19$ pm measured at FWHM (limited by the resolution of the spectrometer). At currents larger than 6.8 A, it is obvious that also emission at other wavelengths occurs. However, due to the small spectral distance from the pronounced line, the emission width is still smaller than $\Delta\lambda_{FWHM} = 80$ pm (1.3 cm^{-1}).

In Fig. 9, we show the spectrum at 6 W plotted on a logarithmic scale. From the figure, it can be seen that an additional lasing

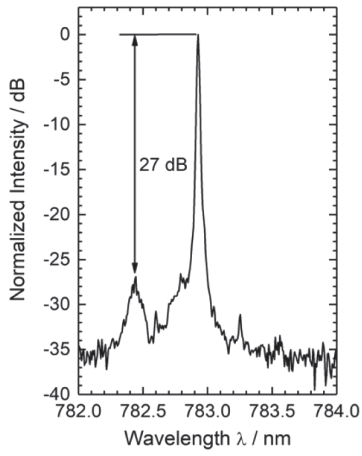

Fig. 9. Emission spectrum for the DBR-tapered laser in Fig. 7 at an output power of $P = 6$ W and $T = 25°C$.

mode occurs at shorter wavelength with a side mode suppression ratio (SMSR) of 27 dB. At lower output powers between 1 W and 5 W, the SMSR is in the range of about 35 dB.

5. BEAM QUALITY

The lateral near field distribution at beam waist position measured at $P = 6$ W is given in Fig. 10. Here, it can be seen that at the beam waist, the measured intensity profile shows a pronounced central lobe together with three sidelobes. Fitting a Gaussian profile (red curve) to the central lobe, a width of this lobe of 3.2 µm (FWHM) is determined, and about 70% of the optical power of the laser originates from this lobe, i.e., 4.2 W output power. For an evaluation of the width measured at $1/e^2$-level, a sidelobe must be considered, which leads to a width of 11.5 µm. Using second moments, the width is 31.3 µm.

The lateral far field has an angle of $\Theta_{1/e2} = 12.5°$ and $\Theta_{2nd} = 15.2°$. Determining the lateral beam propagation ratio M^2_{lat} at $1/e^2$-level at $P = 6$ W, a value of $M^2_{lat-1/e2} = 2.5$ was obtained. $M^2_{lat-2nd}$ was 8.3.

At $P = 6$ W, the astigmatism, i.e., the distance between the two focal planes determined by the front facet and the position of the beam waist, is about 1 mm.

Developments of the lateral beam parameters with output power are compiled in Figs. 11 and 12.

In the figure, it can be seen that the lateral beam waist width increases with output power. From $P = 1$ W to $P = 6$ W, the beam waist width measured at $1/e^2$-level increases from 5 µm to 11.5 µm. This indicates that at higher output power, as shown in Fig. 10, sidelobes increase and become larger than the $1/e^2$-level. The spatial filtering of the unwanted spurious modes deteriorates. The beam waist measured with the second moment method is as expected larger compared to the $1/e^2$-width. Here, the measured value increases from 11.2 µm at 1 W to 31.3 µm at 6 W.

The changes with increasing output power for the lateral far field angle and the differences between the two methods of determination are smaller. The values measured according to the $1/e^2$-level show a weak decrease from about 14° at small powers down to 12.5° at higher power. The value determined with the second moment method is approximately constant at about 15°.

According to the development of the lateral beam waist, also the lateral M^2-values increase with output power. Here, the $M^2_{lat-1/e2}$ increases from 1.2 to 2.5, and the $M^2_{lat-2nd}$ from 2.9 to 8.3.

The astigmatism changes in the studied power range from 860 µm to 1020 µm. This indicates the formation of a thermal lens in the resonator, which might also influence the observed roll-over and the change in spectral behavior at higher output power with a decreasing mode hop distance.

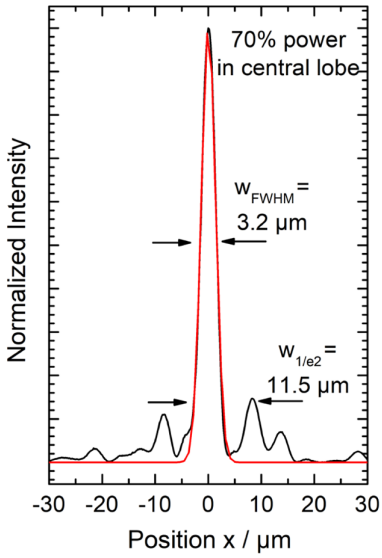

Fig. 10. Near field distribution at beam waist position of the laser in Fig. 7 at an output power of $P = 6$ W and $T = 25°$C. Black, measured data; red, Gaussian fit.

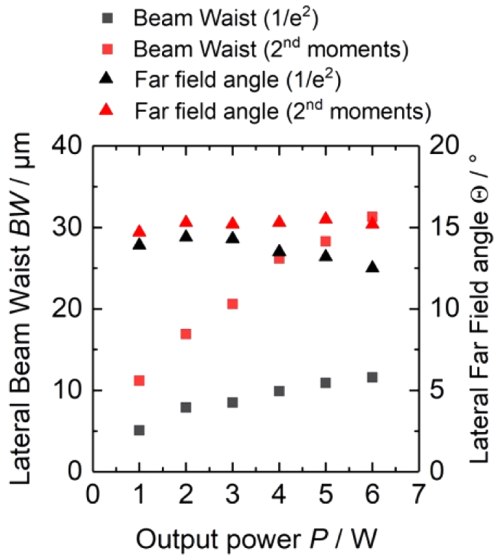

Fig. 11. Lateral beam waist width and far field angle as function of output power.

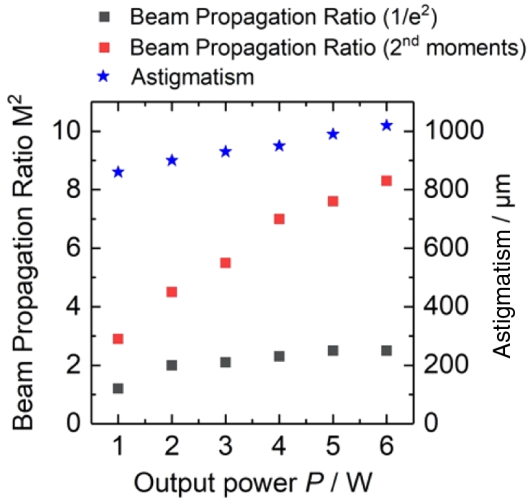

Fig. 12. Lateral beam propagation ratio and astigmatism as function of output power.

6. CONCLUSION

A 783 nm DBR-tapered diode laser with a maximum output power of 7 W is presented. Up to an output power of 6.4 W, almost along the entire operating range of the device, single dominant mode emission is shown with a spectral width below 20 pm. Even in multimode operation, a spectral width below 80 pm is measured. The device shows an emission with lateral beam propagation ratios $M^2_{lat-1/e2} = 2.5$ and $M^2_{lat-2nd} = 8.3$ up to an output power of 6 W. To the best of our knowledge, this is the highest wavelength stabilized output power at this beam quality level. With these features, the device is well suited as a fiber coupled pump module for Tm:YAG lasers and as a laser source for Raman spectroscopy using, e.g., fiber probes and large excitation spot sizes.

The improved features of these devices are due to the implementation of previous knowledge obtained for longer wavelength devices, especially at 1030 nm [17], including the separate excitation of RW and tapered sections, the design of a tapered grating, implantation along the ridge, and improved heat removal.

Funding. Bundesministerium für Bildung und Forschung (16FMD02); Leibniz-Gemeinschaft (SAW-2016-IPHT-2).

Disclosures. The authors declare no conflicts of interest.

Data Availability. Data underlying the results presented in this paper are not publicly available at this time but may be obtained from the authors upon reasonable request.

REFERENCES

1. E. Beyatli and U. Demirbas, "Widely-tunable dual-wavelength operation of Tm:YLF, Tm:LuAG and Tm:YAG lasers using off-surface optic axis birefringent filters," Appl. Opt. **57**, 6679–6686 (2018).
2. W. L. Gao, J. Ma, G. Q. Xie, J. Zhang, D. W. Luo, H. Yang, D. Y. Tang, J. Ma, P. Yuan, and L. J. Qian, "Highly efficient 2 μm Tm:YAG ceramic laser," Opt. Lett. **37**, 1076–1078 (2012).
3. K. Shin and H. Chung, "Wide area coverage Raman spectroscopy for reliable quantitative analysis and its applications," Analyst **138**, 3335–3346 (2013).
4. R. L. McCreery, "Lasers for Raman spectroscopy," in *Raman Spectroscopy for Chemical Analysis*, J. D. Winefordner, ed. (Wiley Interscience, 2000), Vol. **157**, pp. 127–148.
5. Z. P. Qin, J. G. Liu, G. Q. Xie, J. Ma, W. L. Gao, L. J. Qian, P. Yuan, X. D. Xu, J. Xu, and D. H. Zhou, "Spectroscopic characteristics and laser performance of Tm:$CaYAlO_4$ crystal," Laser Phys. **23**, 105806 (2013).
6. L. Bao, M. DeVito, M. Grimshaw, P. Leisher, H. Zhou, W. Dong, X. Guan, S. Zhang, R. Martinsen, and J. Haden, "High performance diode lasers emitting at 780-820 nm," Proc. SPIE **8241**, 824109 (2012).
7. M. Maiwald, G. Erbert, A. Klehr, B. Sumpf, H. Wenzel, T. Laurent, J. Wiedmann, H.-D. Kronfeldt, and H. Schmidt, "Reliable operation of 785 nm DFB diode lasers for rapid Raman spectroscopy," Proc. SPIE **6456**, 64560W (2007).
8. H. Ahmad, B. Sumpf, K. Sowoidnich, A. Klehr, and H.-D. Kronfeldt, "In-situ Raman setup for deep ocean investigations applying two 1000 m optical fiber cables and a 785 nm high power diode laser," Mar. Sci. **2**, 132–138 (2012).
9. K. Inoguchi, H. Kudo, S. Sugahara, S. Ito, H. Yagi, and H. Takiguchi, "Operation of 780 nm AlGaAs distributed feedback lasers at 100C with low-loss waveguide structure," Jpn. J. Appl. Phys. **33**, 852–855 (1994).
10. H. Wenzel, A. Klehr, M. Braun, F. Bugge, G. Erbert, J. Fricke, A. Knauer, M. Weyers, and G. Tränkle, "High-power 783nm distributed-feedback laser," Electron. Lett. **40**, 123–124 (2004).
11. L. Jiang, M. Achtenhagen, N. V. Amarasinghe, P. Young, and G. Evans, "High-power DBR laser diodes grown in a single epitaxial step," Proc. SPIE **7230**, 72301F (2009).
12. B. Sumpf, J. Fricke, M. Maiwald, A. Müller, P. Ressel, F. Bugge, G. Erbert, and G. Tränkle, "Waveguide stabilized 785 nm DBR-ridge waveguide lasers with an output power of 215 mW," Semicond. Sci. Technol. **29**, 045025 (2014).
13. A. Müller, M. Maiwald, and B. Sumpf, "Compact diode laser-based dual-wavelength master oscillator power amplifier at 785 nm," IEEE Photon. Technol. Lett. **31**, 1120–1123 (2019).
14. J. N. Walpole, "Semiconductor amplifiers and lasers with tapered gain regions," Opt. Quantum Electron. **28**, 623–645 (1996).
15. M. Mikulla, P. Chazan, A. Schmitt, S. Morgott, A. Wetzel, M. Walther, R. Kiefer, W. Pletschen, J. Braunstein, and J. Weimann, "High-brightness tapered semiconductor laser oscillators and amplifiers with low-modal gain epilayer-structures," IEEE Photon. Technol. Lett. **10**, 654–656 (1998).
16. B. Sumpf, K.-H. Hasler, P. Adamiec, F. Bugge, F. Dittmar, J. Fricke, H. Wenzel, M. Zorn, G. Erbert, and G. Tränkle, "High-brightness quantum well tapered lasers," IEEE J. Sel. Top. Quantum Electron. **15**, 1009–1020 (2009).
17. A. Müller, C. Zink, J. Fricke, F. Bugge, G. Erbert, B. Sumpf, and G. Tränkle, "Efficient, high brightness 1030 nm DBR tapered diode lasers with optimized lateral layout," IEEE J. Sel. Top. Quantum Electron. **23**, 1501107 (2017).
18. G. Erbert, F. Bugge, A. Knauer, J. Sebastian, A. Thies, H. Wenzel, M. Weyers, and G. Tränkle, "High-power tensile-strained GaAsP-AlGaAs quantum-well lasers emitting between 715 and 790 nm," IEEE J. Sel. Top. Quantum Electron. **5**, 780–784 (1999).
19. A. Knauer, F. Bugge, G. Erbert, H. Wenzel, K. Vogel, U. Zeimer, and M. Weyers, "Optimization of GaAsP/AlGaAs-based QW laser structures for high power 800 nm operation," J. Electron. Mater. **29**, 53–56 (2000).
20. P. Ressel, G. Erbert, U. Zeimer, K. Häusler, G. Beister, B. Sumpf, A. Klehr, and G. Tränkle, "Novel passivation process for the mirror facets of high-power semiconductor diode lasers," IEEE Photon. Technol. Lett. **17**, 962–964 (2005).
21. B. Sumpf, G. Beister, G. Erbert, J. Fricke, A. Knauer, P. Ressel, and G. Tränkle, "Reliable 1-W CW operation of high-brightness tapered diode lasers at 735 nm," IEEE Photon. Technol. Lett. **16**, 984–986 (2004).
22. F. Dittmar, B. Sumpf, J. Fricke, G. Erbert, and G. Tränkle, "High-power 808-nm tapered diode lasers with nearly diffraction-limited beam quality of $M^2 = 1.9$ at $P = 4.4$ W," IEEE Photon. Technol. Lett. **18**, 601–603 (2007).